

Simulating methylamine using symmetry adapted qubit-excitation-based variational quantum eigensolver

Konstantin M. Makushin¹ and Aleksey K. Fedorov²

¹*Kazan Federal University, Kazan 420008, Russia*

²*National University of Science and Technology "MISIS", 119049 Moscow, Russia*

(Dated: January 31, 2025)

Understanding the capabilities of quantum computer devices and estimating the required resources to solve realistic tasks are among the most important problems towards achieving useful quantum computational advantage. In this work, we analyze the resources that are needed to simulate certain molecules on a medium-scale quantum computer with the use of the variational quantum eigensolver (VQE) approach. As the conventional realization of the VQE approach significant amount of resources for simulation, we propose and analyze optimization techniques based on molecular point group symmetries (symmetry adaption) and compact excitation circuits (qubit-excitation-based). These optimizations allows significant reduction of the essential computational capabilities yet ensuring the convergence to the required energies. We first apply this approach for small molecules, such as LiH and BeH₂, to evaluate their compatibility, accuracy, and potential applicability to larger problems. Then we demonstrate that instead of 600,000 two-qubit operations (in the STO-3G basis using a naive version of the Unitary Coupled Cluster ansatz), we are able to simulate methylamine molecules with 26 qubits and about 12,000 of two-qubit gates using our method. We accomplish our analysis by estimating required resources for a formic acid molecule, whose simulation requires about 15,000 of two-qubit gates. Thus, the proposed combination of certain optimization methods can reduce the number of two-qubit operations by several orders of magnitude. Although, we present alternative approaches that are of interest in the context of the further optimization in the number of two-qubit operation, we note that these approaches do not perform well enough in terms of the convergence to required energies. While these challenges persist, our resource analysis represents a valuable step towards the practical use of quantum computers and the development of better methods for optimizing computing resources.

I. INTRODUCTION

A problem of calculating energies and electronic structures of molecular ground and excited states is of primary importance for various industry-relevant problems, such as finding catalysts for chemical reactions and materials design [1]. However, the computational complexity of exact quantum chemistry simulations for many relevant situations grows exponentially with the system size [2]. This problem has stimulated the development of classical approaches that capture relevant chemical properties [3], yet used simplifications may hinder some underlying electronic correlation effects that may play important role for various cases.

To overcome these limitations and address the problem of growing computational demands, the quantum computing paradigm present a promising solution [4–6]. By leveraging the principles of quantum physics, quantum computing devices offer the potential to efficiently solve complex quantum-chemical problems that are intractable for classical computers [5, 6].

There are several approaches to utilize the resources of quantum computing devices to solve computational problems in quantum chemistry. First, special-purpose quantum devices can be used [7]. In particular, boson sampling [8], analog quantum simulators [9], and quantum annealing [10] devices have been used for solving various chemical problems; however, encoding of chemical problems to the setting of special-purpose quantum

computers may hinder the potential quantum computational advantage [11, 12].

Second, universal quantum computing models, specifically, gate-based quantum computers, have the potential to be used for quantum chemistry simulation [4–6]. In order to encode electronic states of molecules into qubits, one uses a basis of predefined *spin-orbitals*, i.e., quantum states that can be occupied by individual electrons. Each qubit in the quantum register represents one such spin-orbital, with its value (0 or 1) determining whether this spin-orbital is occupied or not. The molecular state is then a superposition of multiple occupancy configurations. The quantum computing device is then used, e.g., to find the lowest-energy state of molecules.

However, the full quantum simulation using gate-based quantum computers require prohibitively large amount of resources, specifically, the number of two-qubit operations [5, 6]. The ability to implement two-qubit operations in existing quantum computing devices is limited by the amount of errors due to the effects related to interactions with environment. In this context, the variational quantum eigensolver (VQE) approach [13–16] is of interest since this algorithm can be implemented already with the use of existing noisy intermediate-scale quantum (NISQ) devices. VQE has shown its ability to calculate molecular ground states and energy spectra with chemical accuracy in a number of studies [7, 15–17]. An overview of the developments of VQE showcasing its adaptability and potential for complex quantum

systems is presented in Ref. [7]. For example, the recent study [17] has highlighted the methodological advancements and best practices in applying VQE to quantum chemistry problems, which emphasises its versatility for a variety of molecular systems. VQE has been used in benchmarking studies on a variety of quantum hardware platforms and molecular configurations, see Refs. [18, 19]. Applications of VQE in solving specific tasks, such as applying sophisticated Hamiltonian corrections for molecular simulations or calculating the magnetic properties of rare earth ions, has been demonstrated in Refs. [20, 21]. Large-scale implementations on high-performance supercomputers, which highlights the scalability of VQE for difficult systems, has been studied in Ref. [22]. Recently proposed improvements in the VQE approach include improvements in circuit depth optimization and error mitigation [23] and further reduce computational expenses by using symmetry-compressed double factorization approaches [24]. All of this research supports the idea that VQE is an option for solving quantum-chemical issues that are beyond the capabilities of classical computers, when combined with advancements in algorithmic technology and better quantum hardware. Variational approaches based on VQE have been used to analyze small molecules, such as hydrogen (H_2) [25–27], lithium hydride (LiH) [25, 27], beryllium hydride (BeH_2) [25], and water (H_2O) [28], as well as to simulate diazene isomerizations [29] and carbon monoxide oxidation [16].

Methylamine (CH_3NH_2) and formic acid (CH_2O_2), also known as methanoic acid, are both simple yet fundamental organic compounds in chemistry and biochemistry. Methylamine, an amine related to ammonia, is crucial in manufacturing pesticides, pharmaceuticals, and solvents and constitutes amino acids, which are building blocks of protein [30]. Formic acid, the simplest carboxylic acid, is found in insect stings and is utilized industrially in making leather and textiles, and as a feed preservative. Both play significant roles in biological systems [31], with formic acid also acting as a key metabolic agent and a strong solvent. More precise understanding of their properties and features of compounds on their basis may provide valuable information for various problems chemistry and life sciences.

In this work, we analyze the resources that are needed to simulate certain molecules on a medium-scale quantum computer with the use of the VQE approach taking into account possible optimization. Specifically, we combine the use of molecular point group symmetries (symmetry adaption) and compact excitation circuits (qubit-excitation-based). As we demonstrate, these optimizations allows significant reduction of the essential computational capabilities yet ensuring the convergence to the required energies. First we use this approach for small molecules, such as LiH and BeH_2 , to evaluate their compatibility, accuracy, and potential applicability to larger problems. We then simulate methylamine molecules with 30 qubits and about 12,000 of two-qubit gates using our method, which is the significant gain the terms of re-

quired resources compared to the standard approaches. We accomplish our analysis by estimating required resources for a formic acid molecule, whose simulation requires about 15,000 of two-qubit gates. The inter-nuclear coordinates used in this study have been sourced from the CCCBDB database [32] and optimized at the CCSD(T) level of theory with the Def2TZVPP basis set. Our results demonstrate that these optimization techniques performed well and reduce the circuit depth and the number of two-qubit gates by an order of magnitude making such simulations more feasible using near-term quantum computers.

Our paper is organized as follows. We formulate the problem in Sec. II. In Sec. III, we formulate the VQE approach for solving quantum-chemical problems. In Sec. IV, we analyze the required quantum resourced for simulating methylamine and formic acid molecules using the VQE approach. We take into account possible optimization techniques that can be used to reduce the amount of the required results for VQE-based quantum chemical simulations. We summarize our results and conclude in Sec. V.

II. ELECTRONIC WAVE FUNCTION

In the most general case, the electronic wave function Ψ for a many-body system, such as an N -electron molecule, can be expressed as a *superposition* of multiple Slater determinants as follows:

$$\Psi(\mathbf{x}_1, \dots, \mathbf{x}_N) = \sum_I d_I \mathcal{A} \left\{ \chi_1^{(I)}(\mathbf{x}_1) \chi_2^{(I)}(\mathbf{x}_2) \dots \chi_N^{(I)}(\mathbf{x}_N) \right\}. \quad (1)$$

where $\mathbf{x}_k = (\mathbf{r}_k, \omega_k)$ includes spatial and spin coordinates, $\chi_k(\mathbf{x}_k)$ is a single-electron wave function (spin-orbital), and $\mathcal{A}\{\dots\}$ denotes antisymmetrization (the Slater determinant). The coefficients d_I of the determinants can represent certain variational or combinatorial coefficients. Each individual term in this sum corresponds to a particular electronic configuration of the molecular electronic system (ground state and various excited states).

This generalized representation is valid in the context of the Full Configuration Interaction (FCI) method. However, a full linear combination of determinants is rarely used in practical quantum chemical calculations because the complexity of FCI grows exponentially with the number of electrons and orbitals.

In the context of the VQE approach, the initial approximation often involves a single determinant corresponding to the ground state of the molecular system, which is equivalent to solving the system using the Hartree-Fock method. The wave function (statevector) in this case is

then given by:

$$|\Psi_{\text{HF}}\rangle = \frac{1}{\sqrt{N!}} \begin{vmatrix} \chi_1(\mathbf{x}_1) & \chi_2(\mathbf{x}_1) & \cdots & \chi_N(\mathbf{x}_1) \\ \chi_1(\mathbf{x}_2) & \chi_2(\mathbf{x}_2) & \cdots & \chi_N(\mathbf{x}_2) \\ \vdots & \vdots & \ddots & \vdots \\ \chi_1(\mathbf{x}_N) & \chi_2(\mathbf{x}_N) & \cdots & \chi_N(\mathbf{x}_N) \end{vmatrix}. \quad (2)$$

Each single-electron function (spin-orbital) $\chi_k(\mathbf{r}_k, \omega_k)$ within the determinant can be expressed as a product of two components, where:

1. $\psi_k(\mathbf{r}_k)$ is the *molecular orbital* (MO), which describes the *spatial* distribution of electron density.
2. $\xi_k(\omega_k)$ is one of the two *spin functions* (commonly denoted as α or β), accounting for the possible projections of the electron's spin angular momentum.

Thus, we can write the expression as follows:

$$\chi_k(\mathbf{r}_k, \omega_k) = \psi_k(\mathbf{r}_k) \xi_k(\omega_k). \quad (3)$$

Next, an approximation for the spatial part (MO) of the single-electron spin-orbital using the Linear Combination of Atomic Orbitals (LCAO) method can be used:

$$\psi_k(\mathbf{r}_k) = \sum_{\mu} C_{\mu k} \phi_{\mu}(\mathbf{r}_k), \quad (4)$$

where $\phi_{\mu}(\mathbf{r}_k)$ are atomic orbitals (AOs), and $C_{\mu j}$ are coefficients determined, for example, from the Roothaan equations (Hartree-Fock method). Further representation of AOs depends on the chosen basis set.

The orbitals derived from such approximations serve as *input parameters* for quantum computational algorithms, encoding the electronic structure into a qubit representation. However, for quantum algorithms based on phase estimation, the number of qubits and quantum operations grows rapidly with system size, making them computationally infeasible for the current and foreseen hardware [33]. To address this challenge, hybrid quantum-classical approaches have been introduced [15]. One of the most widely adopted of these is the VQE, which leverages both quantum hardware and classical optimization and is presented in the section below.

III. VQE FORMALISM

During the last decade, a large variety of modifications of the VQE approach have been proposed [15], however the majority of them is based on the Ritz variational principle. The Ritz principle involves choosing a certain parametrized combination of wave functions or state vectors i.e. the *ansatz*, and minimizing the functional defined on this parametrized combination. Choosing the right *ansatz* should take into account the specifics of the problem and its boundary conditions. In other words, the *ansatz* represents a linear combination of some known

functions, which are parameterized by some unknown coefficients:

$$\Psi = \sum_i \theta_i \psi_i. \quad (5)$$

Let \mathcal{H} be the Hamiltonian of a certain physical system, and its spectrum of eigenvalues is bounded from below by the minimum eigenvalue E_0 . Assuming that the state vector $|\Psi\rangle$ can be described using a set of variable parameters $\boldsymbol{\theta} = \{\theta_1, \theta_2, \dots, \theta_i\}$ similarly to Eq. (5), we can approximate the ground state energy of the Hamiltonian by minimizing the following functional, which is expressed with the following inequality:

$$E_0 \leq \frac{\langle \Psi(\boldsymbol{\theta}) | \mathcal{H} | \Psi(\boldsymbol{\theta}) \rangle}{\langle \Psi(\boldsymbol{\theta}) | \Psi(\boldsymbol{\theta}) \rangle}. \quad (6)$$

The *ansatz* always gives an expected value that is greater than or equal to the ground state energy. However, if the chosen *ansatz* is a wave function orthogonal to the ground state wave function, then this method would give an estimate for one of the excited states of the system.

The general idea behind all of VQE-type algorithms boils down to the following. As a first step, it is necessary to define a target function C , which encodes the solution to the problem. Then one has to choose a suitable *ansatz* depending on a discrete or continuous set of parameters $\boldsymbol{\theta}$. After that, one needs to perform optimization of the target function using a classical computer:

$$\boldsymbol{\theta}^* = \arg \min_{\boldsymbol{\theta}} C(\boldsymbol{\theta}) \quad (7)$$

Considering the molecular ground state estimation problem, it is necessary to map the molecular Hamiltonian to the qubit Hamiltonian. Under the Born-Oppenheimer approximation, the molecular Hamiltonian is usually expressed in its second-quantized form:

$$H = \sum_{p,q=1}^M h_{pq} a_p^\dagger a_q + \frac{1}{2} \sum_{p,q,r,s=1}^M g_{pqrs} a_p^\dagger a_r^\dagger a_s a_q, \quad (8)$$

where $a_p^\dagger(a_p)$ is the fermionic creation (annihilation) operator and M is the total number of SOs. The coefficients h_{pq} and g_{pqrs} are called one- and two-electron integrals and can be computed classically.

To transform fermionic operators into qubit operators, several transformations, such as Jordan-Wigner, Parity, and Bravyi-Kitaev, can be used. Qubit operators or Pauli strings, refer to tensor products of Pauli matrices X , Y , Z and an identity operator I that act on qubits. After the transformation is realized, one obtains a qubit Hamiltonian in the form

$$H = \sum_i \beta_i P_i, \quad (9)$$

where P_i are Pauli strings. Each Pauli string can be then measured individually or in commutative groups using additional post-rotation gates, preceded by the same *ansatz* circuit for every Pauli string.

The parametrized ansatz can be chosen based on a completely heuristic approach or on some physical intuition. In the case of quantum chemistry, we can adopt the well-known Unitary Coupled Cluster (UCC) ansatz, which can recover a portion of the electron correlation energy by evolving the Hartree-Fock initial wave function. Using the Hartree-Fock state as a reference, we can write the following expression:

$$|\Psi(\boldsymbol{\theta})\rangle = \hat{U}(\boldsymbol{\theta})|\psi_{HF}\rangle = e^{\hat{T}(\boldsymbol{\theta}) - \hat{T}^\dagger(\boldsymbol{\theta})}|\psi_{HF}\rangle, \quad (10)$$

where $\hat{T}(\boldsymbol{\theta})$ is a parametrized cluster operator and $\hat{U}(\boldsymbol{\theta})$ represents the corresponding unitary ansatz. Usually, only single-electron and double-electron excitations are considered, so:

$$\hat{T}(\boldsymbol{\theta}) = \hat{T}_1(\boldsymbol{\theta}) + \hat{T}_2(\boldsymbol{\theta}). \quad (11)$$

The algorithm for the classical optimization part of VQE should be chosen based on the specifics of a convergence, resource requirements, and noise tolerance for a certain problem. For instance, gradient-based optimizers like BFGS or L-BFGS are often preferred for smooth parameter landscapes due to their fast convergence [34], while derivative-free methods such as COBYLA [35] or SPSA [36] may better handle noisy quantum hardware at the cost of increased circuit evaluations. Additionally, the choice must balance computational overhead with scale of the problem, as iterative algorithms, such as ADAM [37], can adaptively adjust learning rates but may struggle with high-dimensional parameter spaces typical in large molecular systems.

IV. VQE SIMULATIONS

Considering the aforementioned fermionic transformations and the STO-3G basis set, each SO can be encoded with one qubit. Thus, the total number of qubits is equal to the number of SOs: $N_q = M$. For formic acid and methylamine we have 17 and 15 MOs, which correspond to 34 and 30 SOs, or equivalently, to the number of qubits required for each system, respectively.

The number of qubits can be reduced by employing the frozen core approximation, where the inner 1s orbitals of carbon and oxygen in the formic acid molecule and carbon and nitrogen in the methylamine molecule are frozen. This step reduces the required number of qubits by 6 for CH_2O_2 and by 4 for CH_3NH_2 . Additionally, by applying a technique known as *qubit tapering* [38], which exploits the discrete \mathbb{Z}_2 symmetries of the Hamiltonian Pauli strings, we can further eliminate three additional qubits from our simulation for both molecules, resulting in final counts of 25 and 23 qubits.

Utilizing the coordinates in Table I allows us to derive the qubit form of the molecular Hamiltonian (9) and ascertain the number of terms it contains. For molecular Hamiltonians it scales with the number of electrons as

Molecule	Atom	X (Å)	Y (Å)	Z (Å)
Methylamine	C	0.0519020	0.7064670	0.0000000
	N	0.0519020	-0.7615000	0.0000000
	H	-0.9428060	1.1684160	0.0000000
	H	0.5906740	1.0624810	0.8789330
	H	0.5906740	1.0624810	-0.8789330
	H	-0.4566340	-1.1008410	-0.8075530
	H	-0.4566340	-1.1008410	0.8075530
Formic Acid	C	0.0000000	0.3858930	0.0000000
	O	-0.8988900	-0.6261750	0.0000000
	O	1.1799510	0.1951720	0.0000000
	H	-0.4628290	1.3844990	0.0000000
	H	-1.7856570	-0.2518330	0.0000000

Table I. Calculated atomic coordinates for methylamine (CH_3NH_2) and formic acid (CH_2O_2) in angstroms.

$\mathcal{O}(N^4)$. This is a critical factor in determining the requisite number of quantum circuits to be measured at each iteration of VQE algorithm. Besides, we can adopt more sophisticated grouping methods for Pauli terms, such as *qubit-wise* and *general* groupings [39]. These methods leverage the commutative properties of Pauli terms to notably decrease the number of necessary measurements.

In considering the UCC Singles and Doubles (UCCSD) variational ansatz and employing the first-order Suzuki-Trotter decomposition, we aim to quantify the electronic excitations, the depth of the parameterized quantum circuit, and the total number of gates within these circuits. If we consider a system with N electrons and define the number of single excitations as $N_S = N(M - N)$, and the number of double excitations as:

$$N_D = \frac{N(N-1)}{2} \frac{(M-N)(M-N-1)}{2}. \quad (12)$$

Then the total number of one-qubit and two-qubit gates in the ansatz circuit can be approximately estimated as follows:

$$\begin{aligned} N_{1\text{-qubit}} &= \alpha_S N_S + \alpha_D N_D, \\ N_{2\text{-qubit}} &= \beta_S N_S + \beta_D N_D. \end{aligned} \quad (13)$$

where α_S (β_S) is the average number of one-qubit (two-qubit) gates per single excitation and α_D (β_D) is the average number of one-qubit (two-qubit) gates per double excitation.

The total circuit depth can be estimated in the similar way:

$$d = \gamma_S N_S + \gamma_D N_D, \quad (14)$$

where γ_S , γ_D contribution to the circuit depth from each single/double excitation. The coefficients from Eqs. (13) and (14) depend on the actual definition of excitation sub-circuits in the ansatz, the fermionic transformation used, and the number of qubits. Recent papers have presented more optimal ways of constructing such circuits with fewer CNOT gates [40–42].

One could use so-called *qubit excitations*, which always have a fixed number of CNOT gates. However, it is not

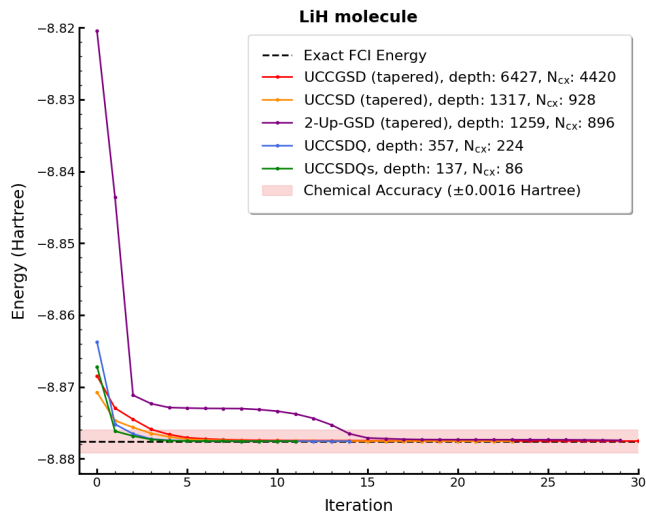


Figure 1. VQE calculation for the LiH molecule using various types of ansatzes and optimization methods. The plot compares the convergence of energy values with the FCI energy as a reference and indicates the chemical accuracy threshold, N_{cx} represents the number of two-qubit gates.

clear whether they can adequately account for the electronic correlation contribution, as they ignore the anti-commutation of fermions by excluding Pauli Z products from the operator exponent.

A naive implementation of the UCCSD ansatz leads to excessive resource requirements since the circuit depth (14) is proportional to the number of two-qubit gates which scales as $\sim \mathcal{O}(N^4)$. However, one can employ several techniques to slightly reduce these requirements. One of them is k-UpCCGSD (for brevity k-UpGSD) [43, 44] ansatz, where k stands for the number of repetitions of UpCCGSD ansatz with the new set of variational parameters for each repetition.

The main difference from UCCSD is that it includes only two-body terms, which shift pairs of opposite-spin electrons from fully occupied to completely unoccupied spatial orbitals making sure there are no singly occupied states described. The estimated circuit parameters for this method are presented in Table II. Its combination with the *qubit excitations* approach was also evaluated and is shown in the same table. However, the *qubit tapering* procedure was not applied to *qubit excitations* due to incompatibilities between these methods.

An alternative way to optimize the UCCSD ansatz is to filter out the excitation terms by their irreducible representations [45]. In other words, one should retain only those terms whose irreducible representations coincide with the irreducible representation of the target state. It is presented in combination with the previous methods as k-UpGSDQs in Table II. Moreover, the use of the Bravyi-Kitaev mapping could result in fewer two-qubit operations count due to lower Pauli-weight [46], i.e. the maximum number of non-identity operators in any Pauli

string produced by the mapping, in some cases it can improve scaling of Eq. (13).

For the current resource estimations, an in-house quantum chemistry library was utilized, specifically developed for the efficient implementation of variational quantum algorithms [47]. First, to make sure the chosen ansatz construction methods and optimization techniques work as expected, we tested them on two relatively simple molecules, LiH and BeH₂, both with a small number of SO (STO-3G basis suggested for both molecules). For LiH, we consider freezing the inner 1s orbital, which resulted in 10 qubits in the non-tapered regime and 6 in the tapered regime. For BeH₂, we initially have 14 qubits; the frozen core method reduced this to 12 qubits in the non-tapered regime and 7 qubits with tapering. We then calculate their ground state energies using the VQE and compared the results for different ansatz types. For both molecules, we use a noiseless statevector simulator in the combination with the BFGS algorithm for classical optimization.

We present the results of VQE calculations for the LiH molecule in Fig. 1. The plot shows how the energy converged over iterations for various ansatz types, such as UCCGSD, UCCSD, 2-Up-GSD, UCCSDQ, and UCCSDQs. The dashed black line represents the exact FCI energy, which we used as a reference. The shaded area around it shows the chemical accuracy threshold of ± 0.0016 Hartree. Among all the ansatz types, UCCSDQs demonstrates the best performance: it achieves the lowest circuit depth (137) and two-qubit gate count (86), while still maintaining chemical accuracy.

In Fig. 2, we present the same analysis for the BeH₂ molecule. Again, one can see how each ansatz converged to the ground state energy. As in the case of the LiH simulation, UCCSDQs proves to be the most resource-efficient, as it requires the least resources (circuit depth of 279 and two-qubit gate count of 190), while staying within the chemical accuracy range. The energy curves initially drop sharply and then level off as they approach the exact FCI value, highlighting the efficiency of these methods for BeH₂.

Overall, these results show that the methods that we use perform well for calculating ground state energies of small molecules like LiH and BeH₂. They also highlight how different ansatz types can affect the balance between accuracy and resource needs. While these methods perform great for smaller systems, scaling them up to larger molecules is a whole different challenge.

Indeed, as shown in Table II, which gives resource estimates for more complex molecules, such as methylamine and formic acid, the computational demands become significant. Even with the STO-3G minimal basis set, the required circuit depth and number of qubits for these molecules are way beyond what current quantum hardware can handle. Alternative methods for constructing the ansatz, such as *adaptive ansatzes* (ADAPT-VQE) [16, 48] or *evolutionary algorithms* [49], can reduce the computational resources, for example by shortening

Parameter	CH ₃ NH ₂					CH ₂ O ₂				
	UCCSD	UpGSD	UCCSDQs	UpGSDQ	UpGSDQs	UCCSD	UpGSD	UCCSDQs	UpGSDQ	UpGSDQs
Ansatz Type	UCCSD	UpGSD	UCCSDQs	UpGSDQ	UpGSDQs	UCCSD	UpGSD	UCCSDQs	UpGSDQ	UpGSDQs
Circuit Depth	514379	14758	5766	473	247	563722	15026	7563	514	266
Qubits	23	23	26	26	26	25	25	28	28	28
Total Gates	631022	18526	11558	2822	1526	682524	19466	14610	3294	1638
Two-qubit gates	457800	12896	4130	1014	546	510426	13520	5221	1183	585
Pauli Terms	20908	20908	20908	20908	20908	30423	30423	30423	30423	30423
Circuits	4144	4144	4144	4144	4144	5103	5103	5103	5103	5103
Double Excitations	2394	78	314	78	42	2745	91	397	91	45
Tapering	Yes	Yes	No	No	No	Yes	Yes	No	No	No

Table II. Estimated resources for the VQE computation of CH₃NH₂ and CH₂O₂ molecules. The number of qubits is calculated using the frozen core approximation and the qubit tapering procedure. The number of circuits is based on qubit-wise operator grouping. Parameters for the k-UpGSD, k-UpGSDQ, and k-UpGSDQs ansatzes are estimated with $k = 1$. The best-performing method in terms of the trade-off between required resources and VQE convergence to the FCI energy is highlighted in bold.

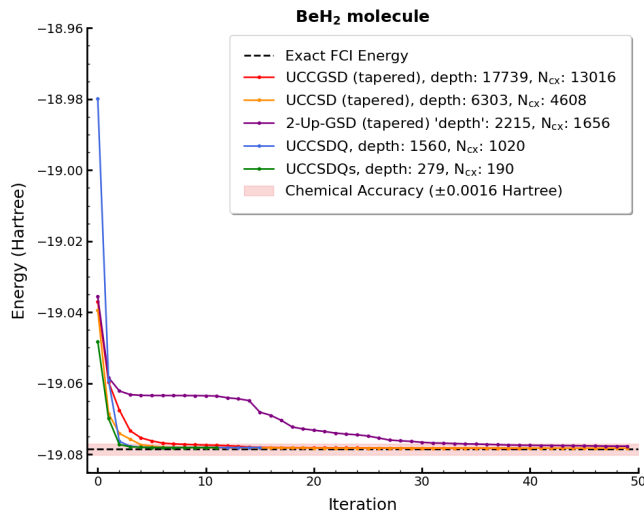


Figure 2. VQE calculation for the BeH₂ molecule using various types of ansatzes and optimization methods. The plot compares the convergence of energy values with the FCI energy as a reference and indicates the chemical accuracy threshold, N_{cx} represents the number of two-qubit gates.

the circuit depth or reducing the total number of variational parameters. However, these methods can incur a higher cost in terms of the number of circuit measurements, because each step in the adaptive or evolutionary procedure often requires extra loops and operator gradient evaluations.

Hence, if we let K be the total number of ADAPT-VQE iterations and P be the operator pool size, the naive measurement cost can scale as

$$\mathcal{O}(K \times P) \quad (15)$$

in *gradient evaluations*, where each gradient evaluation might involve an *inner* VQE with potentially many measurements. If each VQE step needs M_{VQE} measurements for its Hamiltonian estimation, and each gradient check does m param-shift or finite-difference evaluations, we might end up with

$$\mathcal{O}(K \times P \times m \times M_{VQE}) \quad (16)$$

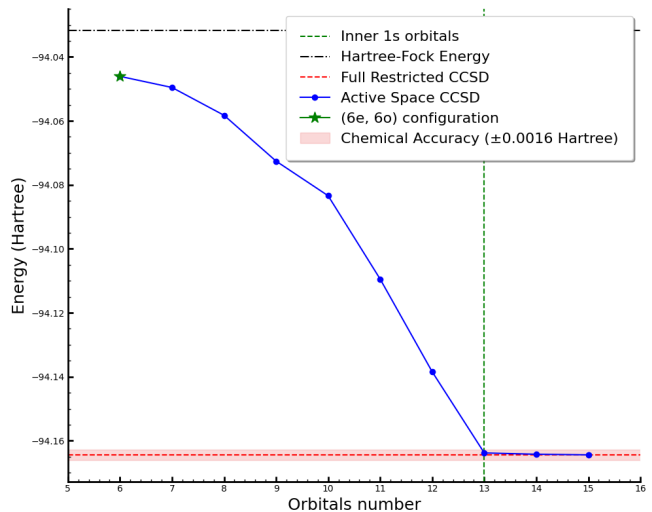


Figure 3. The ground-state energy for different active spaces of the methylamine molecule is shown. The green star indicates the active space configuration used in the VQE calculation. The green vertical line marks the active space region where only the core orbitals are frozen.

as a rough total measurement scaling. In terms of the number of qubits, each of these multiples is proportional to N_q raised to some power α , so the total number of measurements scales polynomially, $\mathcal{O}(N_q^\alpha)$.

The use of more complex bases that allow achieving better description of valence orbitals or account for polarization effects and electron system correlations in molecules, such as 6-31g, 6-31g*, or cc-pVDZ, is associated with similar difficulties. All of them imply that significantly more qubits are required compared to the case of the minimal basis. For instance, simulating the H₄ molecule using the cc-pVDZ basis would require 40 qubits [50]. For simulating the H₂O molecule in the 6-31g basis, 50 qubits are needed. For methylamine and formic acid molecules the number of qubits exceed 60 in the case of complex bases.

Recent studies employing density matrix embedding methods in conjunction with the VQE algorithm demon-

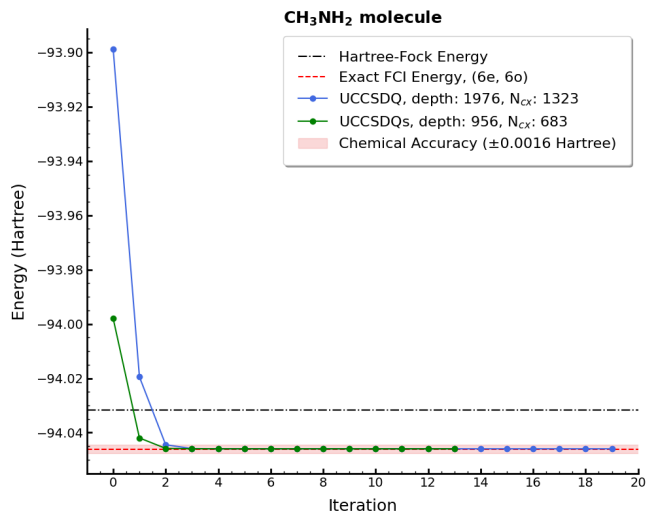


Figure 4. VQE calculation for the CH_3NH_2 molecule in (6e, 6o) active space using UCCSDQ and UCCSDQs ansatzes. The plot compares the convergence of energy values with the FCI energy as a reference and indicates the chemical accuracy threshold, N_{cx} represents the number of two-qubit gates.

strate the simulation of relatively large systems with small computational resources. For instance, the simulation of the C_{18} molecule (a model system consisting of 144 spin orbitals and 72 electrons) has been conducted on a 16-qubit system [51]. The simulation of the torsional barrier of ethane and the quantification of protein-ligand interactions has been demonstrated [52], and the comparison of the use of High-Performance Computing and Matrix Product States for the ansatzes has been presented. Despite the size of the electronic systems in such studies, they often employ the HOMO-LUMO approach to reduce the active space of available orbitals. This leads to a more compact system representation in terms of qubits but comes at the cost of additional error.

We demonstrate the results of simulations for the Methylamine molecule with a restricted number of spin orbitals. We take an active space of 6 electrons and 6 spin orbitals from the full 15 spin-orbital space. First, we will show the energy difference for such a choice. In Fig. 3, one can observe different configurations of the methylamine active space and their corresponding energies. This choice of active space reduces the number of qubits needed for the molecular system. However, when the number of spin orbitals decreases, the calculated energy becomes closer to the Hartree-Fock results. The chemical accuracy is achieved only when the core 1s orbitals are frozen.

For the (6e, 6o) active space configuration of methylamine we use the UCCSDQ and UCCSDQs ansatzes in VQE calculation and the same minimal basis STO-3G. As it shown in Fig 4 the energy converged to the FCI value for both ansatzes. This result shows that for 12-qubit methylamine active space VQE in combina-

tion with aforementioned combination of the optimization methods could achieve the chemical accuracy within small number of iterations. Other types of ansatzes were not tested due to worser computational cost.

The VQE calculation for the formic acid molecule in a reduced active space, similar to the one performed for the methylamine, did not show good convergence to the expected ground state energy. The reason might lie in the stronger electronic correlations between carbon and oxygen atoms in the formic acid, which could not be adequately modeled by circuits based on *qubit excitations*. It is possible that effective fermionic excitation circuits, as proposed in Ref. [40], could achieve better performance, however at the cost of an increased two-qubit gate count.

V. CONCLUSIONS

Quantum chemistry is one of the most interesting avenues for applications of quantum computing devices. In this work, we have presented the results of the computational resources analysis for certain molecules, such as formic acid and methylamine. We have considered the VQE approach and its various extensions as the primary method for quantum chemical simulation.

In order to illustrate the VQE approach, we have demonstrated energy spectra calculations for small molecules, such as LiH and BeH₂, and for methylamine with restricted active space of spin orbitals, all in the minimal basis. Our analysis has shown that the combination of *qubit excitations* with filtration by irreducible representations (UCCSDQs) could drastically decrease the ansatz depth and the number of two-qubit gates, while still recovering the major part of the correlation energy. Combining these methods with the qubit tapering procedure could lead to further improvements; however, it requires a more careful analysis of the connection between \mathbb{Z}_2 symmetries and the representation of the excitation operator circuit, which is beyond the scope of this study. The k-UpCCGSD ansatz could result in smaller improvements, but it can be easily combined with *qubit tapering*. Its combination with irreducible representation filtering showed poor convergence. The ability of these ansatzes to avoid barren plateaus [53] was not investigated in our study. A possible scenario is that, as the number of qubits increases, the process of classical optimization could become stuck in local minima, in the case of the k-UpCCGSD ansatz it could potentially be fixed by increasing k , i.e., by increasing the number of variational parameters.

The quality of two-qubit operations in quantum computing devices is a crucial bottleneck in the real-world application of quantum chemical simulations, e.g. with the use of the using naive UCCSD ansatzes. We have considered possible ways for overcoming this challenges by modifying the algorithmic approach. For example, the combination of k-UpUCCGSD with *qubit excitations* can significantly decrease the circuit depth and the number

of two-qubit gates. The addition of irreducible representation filtering (k-UpGSDQs) could further almost halve the costs. However, the ability to achieve accurate results with these combinations for methylamine and formic acid in the full active space of spin orbitals remains a subject for further study.

As we expect, further improvements in ansatz design,

gate fidelity, and error mitigation may greatly lessen these restrictions and open the door for real-world uses of quantum algorithms like VQE in quantum chemistry.

Acknowledgments. A.K.F. acknowledges the support from the Priority 2030 program at the NIST “MIS” under the project K1-2022-027.

-
- [1] T. Helgaker, P. Jørgensen, and J. Olsen, *Molecular Electronic-Structure Theory* (Wiley, 2000).
- [2] J. Kempe, A. Kitaev, and O. Regev, *SIAM Journal on Computing* **35**, 1070 (2006).
- [3] W. F. van Gunsteren and C. Oostenbrink, *Journal of Chemical Information and Modeling* **64**, 6281 (2024).
- [4] S. Lloyd, *Science* **273**, 1073 (1996).
- [5] Y. Cao, J. Romero, J. P. Olson, M. Degroote, P. D. Johnson, M. Kieferová, I. D. Kivlichan, T. Menke, B. Peropadre, N. P. D. Sawaya, S. Sim, L. Veis, and A. Aspuru-Guzik, *Chemical Reviews* **119**, 10856 (2019).
- [6] S. McArdle, S. Endo, A. Aspuru-Guzik, S. C. Benjamin, and X. Yuan, *Rev. Mod. Phys.* **92**, 015003 (2020).
- [7] D. A. Fedorov, B. Peng, N. Govind, and Y. Alexeev, *Materials Theory* **6**, 2 (2022).
- [8] J. Huh, G. G. Guerreschi, B. Peropadre, J. R. McClean, and A. Aspuru-Guzik, *Nature Photonics* **9**, 615 (2015).
- [9] J. Argüello-Luengo, A. González-Tudela, T. Shi, P. Zoller, and J. I. Cirac, *Nature* **574**, 215 (2019).
- [10] M. Streif, F. Neukart, and M. Leib, in *Quantum Technology and Optimization Problems*, edited by S. Feld and C. Linnhoff-Popien (Springer International Publishing, Cham, 2019) pp. 111–122.
- [11] R. Xia, T. Bian, and S. Kais, *The Journal of Physical Chemistry B* **122**, 3384 (2018).
- [12] D. A. Chermoshentsev, A. O. Malyshev, M. Esencan, E. S. Tiunov, D. Mendoza, A. Aspuru-Guzik, A. K. Fedorov, and A. I. Lvovsky, “Polynomial unconstrained binary optimisation inspired by optical simulation,” (2022), [arXiv:2106.13167 \[quant-ph\]](https://arxiv.org/abs/2106.13167).
- [13] A. Peruzzo, J. McClean, P. Shadbolt, M.-H. Yung, X.-Q. Zhou, P. J. Love, A. Aspuru-Guzik, and J. L. O’Brien, *Nature Communications* **5**, 4213 (2014).
- [14] J. R. McClean, J. Romero, R. Babbush, and A. Aspuru-Guzik, *New Journal of Physics* **18**, 023023 (2016).
- [15] M. Cerezo, A. Arrasmith, R. Babbush, S. C. Benjamin, S. Endo, K. Fujii, J. R. McClean, K. Mitarai, X. Yuan, L. Cincio, and P. J. Coles, *Nature Reviews Physics* **3**, 625 (2021).
- [16] M. Sapova and A. Fedorov, *Communications Physics* **5**, 199 (2022).
- [17] J. Tilly, H. Chen, S. Cao, D. Picozzi, K. Setia, Y. Li, E. Grant, L. Wossnig, I. Rungger, G. H. Booth, and J. Tennyson, *Physics Reports* **986**, 1 (2022).
- [18] A. Bentellis, A. Matic-Flierl, C. B. Mendl, and J. M. Lorenz, in *2023 IEEE International Conference on Quantum Computing and Engineering (QCE)*, Vol. 1 (IEEE, 2023) pp. 518–523.
- [19] J. Hu, J. Li, Y. Lin, H. Long, X.-S. Xu, Z. Su, W. Zhang, Y. Zhu, and M.-H. Yung, [arXiv preprint arXiv:2211.12775](https://arxiv.org/abs/2211.12775) (2022).
- [20] H. Singh, S. Majumder, and S. Mishra, “Sharv-qe: Simplified hamiltonian approach with refinement and correction enabled variational quantum eigensolver for molecular simulation,” (2024), [arXiv:2407.12305 \[quant-ph\]](https://arxiv.org/abs/2407.12305).
- [21] K. Makushin and E. Baibekov, *Magnetic Resonance in Solids* **25**, 23204 (2023).
- [22] H. Shang, L. Shen, Y. Fan, Z. Xu, C. Guo, J. Liu, W. Zhou, H. Ma, R. Lin, Y. Yang, *et al.*, in *SC22: International Conference for High Performance Computing, Networking, Storage and Analysis* (IEEE, 2022).
- [23] D. S. Steiger, T. Häner, S. N. Genin, and H. G. Katzgraber, [arXiv preprint arXiv:2404.10047](https://arxiv.org/abs/2404.10047) (2024).
- [24] D. Rocca, C. L. Cortes, J. F. Gonthier, P. J. Ollitrault, R. M. Parrish, G.-L. Anselmetti, M. Degroote, N. Moll, R. Santagati, and M. Streif, *Journal of Chemical Theory and Computation* (2024).
- [25] A. Kandala, A. Mezzacapo, K. Temme, M. Takita, M. Brink, J. M. Chow, and J. M. Gambetta, *Nature* **549**, 242 (2017).
- [26] P. J. J. O’Malley, R. Babbush, I. D. Kivlichan, J. Romero, J. R. McClean, R. Barends, J. Kelly, P. Roushan, A. Tranter, N. Ding, B. Campbell, Y. Chen, Z. Chen, B. Chiaro, A. Dunsworth, A. G. Fowler, E. Jeffrey, E. Lucero, A. Megrant, J. Y. Mutus, M. Neeley, C. Neill, C. Quintana, D. Sank, A. Vainsencher, J. Wenner, T. C. White, P. V. Coveney, P. J. Love, H. Neven, A. Aspuru-Guzik, and J. M. Martinis, *Phys. Rev. X* **6**, 031007 (2016).
- [27] C. Hempel, C. Maier, J. Romero, J. McClean, T. Monz, H. Shen, P. Jurcevic, B. P. Lanyon, P. Love, R. Babbush, A. Aspuru-Guzik, R. Blatt, and C. F. Roos, *Phys. Rev. X* **8**, 031022 (2018).
- [28] Y. Nam, J.-S. Chen, N. C. Pienti, K. Wright, C. Delaney, D. Maslov, K. R. Brown, S. Allen, J. M. Amini, J. Apisdorf, K. M. Beck, A. Blinov, V. Chaplin, M. Chmielewski, C. Collins, S. Debnath, K. M. Hudek, A. M. Ducore, M. Keesan, S. M. Kreikemeier, J. Mizrahi, P. Solomon, M. Williams, J. D. Wong-Campos, D. Moehring, C. Monroe, and J. Kim, *npj Quantum Information* **6**, 33 (2020).
- [29] F. Arute, K. Arya, R. Babbush, D. Bacon, J. C. Bardin, R. Barends, S. Boixo, M. Broughton, B. B. Buckley, D. A. Buell, B. Burkett, N. Bushnell, Y. Chen, Z. Chen, B. Chiaro, R. Collins, W. Courtney, S. Demura, A. Dunsworth, E. Farhi, A. Fowler, B. Foxen, C. Gidney, M. Giustina, R. Graff, S. Habegger, M. P. Harrigan, A. Ho, S. Hong, T. Huang, W. J. Huggins, L. Ioffe, S. V. Isakov, E. Jeffrey, Z. Jiang, C. Jones, D. Kafri, K. Kechedzhi, J. Kelly, S. Kim, P. V. Klimov, A. Korotkov, F. Kostritsa, D. Landhuis, P. Laptev, M. Lindmark, E. Lucero, O. Martin, J. M. Martinis, J. R. McClean, M. McEwen, A. Megrant, X. Mi, M. Mohseni, W. Mroczkiewicz, J. Mutus, O. Naaman, M. Neeley, C. Neill, H. Neven, M. Y. Niu, T. E. O’Brien, E. Ostby,

- A. Petukhov, H. Putterman, C. Quintana, P. Roushan, N. C. Rubin, D. Sank, K. J. Satzinger, V. Smelyanskiy, D. Strain, K. J. Sung, M. Szalay, T. Y. Takeshita, A. Vainsencher, T. White, N. Wiebe, Z. J. Yao, P. Yeh, and A. Zalcman, *Science* **369**, 1084 (2020).
- [30] Y. Wu, Z. Jiang, Z. Lin, Y. Liang, and H. Wang, *Nature Sustainability* **4**, 1 (2021).
- [31] A. K. Fedorov and M. S. Gelfand, *Nature Computational Science* **1**, 114 (2021).
- [32] R. D. J. III, “Nist computational chemistry comparison and benchmark database,” NIST Standard Reference Database Number 101, Release 22 (2022), available online: <http://cccbdb.nist.gov/>.
- [33] M. Reiher, N. Wiebe, K. M. Svore, D. Wecker, and M. Troyer, *Proceedings of the national academy of sciences* **114**, 7555 (2017).
- [34] A. Kandala, A. Mezzacapo, K. Temme, M. Takita, M. Brink, J. M. Chow, and J. M. Gambetta, *Nature* **549**, 242 (2017).
- [35] M. J. Powell, *Mathematical Programming* **97**, 605 (2003).
- [36] S. Bravyi, S. Sheldon, A. Kandala, D. C. McKay, and J. M. Gambetta, *PRX Quantum* **2**, 040326 (2021).
- [37] M. Cerezo, A. Arrasmith, R. Babbush, S. C. Benjamin, S. Endo, K. Fujii, J. R. McClean, K. Mitarai, X. Yuan, L. Cincio, *et al.*, *Nature Reviews Physics* **3**, 625 (2021).
- [38] S. Bravyi, J. Gambetta, A. Mezzacapo, and K. Temme, *arXiv* (2017), *arXiv: Quantum Physics*.
- [39] P. Gokhale, O. Angiuli, Y. Ding, K. Gui, T. Tomesh, M. Suchara, M. Martonosi, and F. T. Chong, in *2020 IEEE International Conference on Quantum Computing and Engineering (QCE)* (IEEE, 2020) pp. 379–390.
- [40] Y. S. Yordanov, D. R. Arvidsson-Shukur, and C. H. Barnes, *Physical Review A* **102**, 062612 (2020).
- [41] Y. S. Yordanov, V. Armaos, C. H. Barnes, and D. R. Arvidsson-Shukur, *Communications Physics* **4**, 228 (2021).
- [42] I. Magoulas and F. A. Evangelista, *Journal of Chemical Theory and Computation* **19**, 4815 (2023).
- [43] J. Lee, W. J. Huggins, M. Head-Gordon, and K. B. Whaley, *J. Chem. Theory Comput.* **15**, 311 (2018).
- [44] H. G. Burton, D. Marti-Dafcik, D. P. Tew, and D. J. Wales, *npj Quantum Information* **9**, 75 (2023).
- [45] C. Cao, J. Hu, W. Zhang, X. Xu, D. Chen, F. Yu, J. Li, H.-S. Hu, D. Lv, and M.-H. Yung, *Physical Review A* **105**, 062452 (2022).
- [46] J. T. Seeley, M. J. Richard, and P. J. Love, *The Journal of chemical physics* **137** (2012).
- [47] K. Makushin, M. Sapova, and A. Fedorov, in *Journal of Physics: Conference Series*, Vol. 2701 (IOP Publishing, 2024) p. 012032.
- [48] H. Grimsley, S. Economou, E. Barnes, and et al., *Nat Commun* **10**, 3007 (2019).
- [49] D. Chivilikhin, A. Samarin, V. Ulyantsev, I. Iorsh, R. Oganov, and O. Kyriienko, “Mog-vqe: Multiobjective genetic variational quantum eigensolver,” (2020), *arXiv: Quantum Physics*.
- [50] C. Guo, Y. Fan, Z. Xu, and H. Shang, *Quantum* **7**, 1192 (2023).
- [51] W. L. et al., *Chemical Science* **13**, 8953 (2021).
- [52] H. Shang, Y. Fan, and L. S. et al., *npj Quantum Information* **9** (2023).
- [53] S. Wang, E. Fontana, M. Cerezo, K. Sharma, A. Sone, L. Cincio, and P. J. Coles, *Nature communications* **12**, 6961 (2021).